Analyst

Accepted Manuscript

ROYAL SOCIETY OF CHEMISTRY

www.rsc.org/analyst

Analyst RSCPublishing

PAPER

High throughput and multiplex localization of proteins and cells for in situ micropatterning using pneumatic microfluidics†

Cite this: DOI: 10.1039/x0xx00000x

Received 00th January 2012,
Accepted 00th January 2012

DOI: 10.1039/x0xx00000x

www.rsc.org/

Jian-Chun Wang,[a,b] Wenming Liu,[a] Qin Tu,[a] Chao Ma,[a] Lei Zhao,[a] Yaolei Wang,[a] Jia Ouyang,[c] Long Pang[a] and Jinyi Wang[a,*]

Micropatterning technologies are emerging as an enabling tool for various microfluidics-based applications in life science. However, the high throughput and multiplex localization of multiple bio-components in a microfluidic device has not yet been well established. In this paper, we described a simple and in situ micropatterning method using an integrated microfluidic device with pneumatic microstructures (PμSs) for highly controllable immobilization of both proteins and cells in a high throughput, geometry-dynamic, and multi-patterning way. The precise Pluronic F127 passivation of microchamber surface except the PμSs-blocked regions was performed and characterized, and spatial dynamics and consistency of both the PμSs and protein/cell micropatterning were optically evaluated and quantitatively demonstrated too. Furthermore, a systematical investigation of PμSs-assisted micropatterning in microfluidics was carried out. The feature of high throughput and spatial control of micropatterning can be simply realized by using the well-designated PμS arrays. Meanwhile, co-micropatterning of different proteins (bovine serum albumin and chicken egg albumin) and cells (human umbilical vein endothelial cells and human hepatocellular carcinoma cells) in a microfluidic device was successfully accomplished with the orderly serial manipulation of PμS groups. We demonstrate that PμSs-assisted micropatterning can be applied as a convenient microfluidic component for large-scale and diversified protein/cell patterning and manipulation, which could be useful for cell-based tissue organization, high-throughput imaging, protein-related interactions and immunoassays.

Introduction

Micropatterning technology is always interesting in the application of biochemistry, cellular and molecular biology /immunology.[1,2] This is because of its remarkable capability in precise manipulation of cells, biomolecules (e.g., proteins and nucleic acids), and signal-mediated communication and interaction at microscale.[3-5] Selective arrangement of these biological substances on the designated surface of substrates has gained tremendous attention in fundamental cell research,[2,6] and also open doors to experimental approaches in biomedical diagnostics, drug discovery, and tissue engineering.[7-9] For example, recent progresses in cellular and biomolecular micropatterning have already proven invaluable in increasing our understanding of the structural and functional relationships of homo/heterotopically biological communities.[10-12] In the past decade, a wide variety of micropatterning strategies, such as photolithography,[13] stencil patterning,[14] microfluidic patterning,[15] microcontact printing,[16] ink-jet printing[17] and selective plasma etching,[18] have been explored and proposed for the development and innovation of this microcontrol system in a high throughput and geometry-controllable manner. Nevertheless, the multifactor organization and serial manipulation of micropatterning for the dynamic purpose is still being explored, and it requires a systematic consideration of the bio-microenvironment construction.[19-22]

Microfluidics is supposed to be a promising platform for life science due to its excellent performance in the spatiotemporal control of microfluidic perfusion and biological samples, in simulation of tissue-relevant context, as well as in the feasible sequential manipulation.[23-26] Given the scales at which micropatterning operates, integration with microfluidics can broaden the range of biological applications.[27] However, integrating aforementioned micropatterning methods with microfluidic systems is not straightforward.[28,29] The micropatterning surfaces are commonly incompatible with

microfluidic device assembly because of the harsh treatments (i.e., thermal and plasma bonding) could alter the properties and functionalities of the micropatterning surfaces, or even compromise bioactivity of proteins and cells.[30] Therefore, the development of in situ micropatterning within microfluidic device is potentially of benefit. On the other hand, the continuously increasing complexity of microfluidic systems also requires the development of methods for the robust fabrication and control of the functional surfaces.[31,32] Currently, several approaches like laminar flow micropatterning have been demonstrated to successfully control the surface properties and cell adhesion in microchannels.[33,34] Furthermore, in situ microfluidic protein capture has been developed with the pressure-modulated microfluidic valves.[35,36] However, either the spatial control (e.g., geometry- and size-variable) and high throughput, or the multiple bio-component localization (i.e., different types of proteins and cells) of micropatterning in microfluidics remains largely out of reach.

To this end, we present an in situ micropatterning development of both proteins and cells through the pneumatic microstructures (PμSs) and PμS-assisted surface passivation. The localized proteins and cells with various quantities can be arranged in the microchamber based on the adjustable actuation of PμSs. Moreover, high-throughput and geometry-controlled micropatterning of multiple biological components can be realized in the device respectively using the specially designed PμS arrays. In addition, we demonstrated that this approach has the ability to complete a co-micropatterning of different proteins/cells with an organized localization simultaneously in the same chamber through a successive manipulation of the PμSs.

Experimental

Materials and reagents

RTV 615 poly(dimethylsiloxane) (PDMS) prepolymer and curing agent were purchased from Momentive Performance Materials (Waterford, NY, USA). Surface-oxidized silicon wafers were obtained from Shanghai Xiangjing Electronic Technology Ltd (Shanghai, China). The AZ 50XT photoresist and developer were bought from AZ Electronic Materials (Somerville, NJ, USA). The SU-8 2025 photoresist and developer were purchased from Microchem (Newton, MA, USA). Chicken egg albumin (CEA) was purchased from Dingguo Biotechnology Ltd. (Beijing, China). Bovine serum albumin (BSA) was obtained from Amresco (Solon, OH, USA). The EZ-Label FITC Protein Labeling Kit was brought from Pierce Biotechnology (Rockford, IL, USA). The Alexa Fluro594 Protein Labeling Kit was from Molecular Probes (Eugene, OR, USA). Collagen-I, fluorescein diacetate (FDA), acridine orange (AO), propidium iodide (PI) and Pluronic F127 were bought from Sigma-Aldrich (MO, USA). Dulbecco's modified Eagle's medium (DMEM), fetal bovine serum (FBS), CellTracker Orange CMRA and CellTracker Green CMFDA were obtained from Gibco Invitrogen Corporation (CA, USA). All solutions and other chemicals were purchased from local commercial suppliers and were of analytical reagent grade, unless otherwise stated. All solutions were prepared using ultrapurified water supplied by a Milli-Q system (Millipore®).

Device fabrication

The microfluidic device used in the present study was fabricated through multilayer soft lithography.[37-39] Two different molds were first produced by photolithographic processes to create the fluidic components and control components. The components were embedded in corresponding layer of the PDMS matrix. To prepare the mold for the fabrication of the fluidic components, a 30 μm-thick positive photoresist (AZ 50XT) was spin-coated onto a silicon wafer. After UV exposure, the fluidic components on the wafer were developed using an AZ 400K developer. The mold of the control channels, including the patterning PμSs, was made from a 20 μm-thick negative photoresist (SU8-2025) patterned on a silicon wafer.

Both the fluidic and control molds were exposed to trimethylchlorosilane vapor for 3 min before fabricating the microfluidic device. A well-mixed PDMS prepolymer [RTV 615 A and B (8:1, w/w)] was poured onto the fluidic mold, which was then placed in a Petri dish to obtain a 3 mm-thick fluidic layer. The PDMS prepolymer [RTV 615 A and B (20:1, w/w)] was spin-coated onto the control mold at 1,800 rpm for 60 s to obtain a thin control layer (about 41 μm-thickness). Both layers were cured at 80 ^{o}C for 30 min. After incubation, the fluidic layer was peeled off the mold and holes were introduced for sample access and waste exclusion. Then, the fluidic layer was trimmed, cleaned, and manually aligned to the control mold. After baking at 80 ^{o}C for 2 h, the assembled layers were trimmed, and then peeled off the control mold, and a set of holes were punched to enable access to the control channel network. The punching process was performed using a custom-made puncher with the assistance of TV monitor. The assembled layers were then placed on a glass slide which was spin-coated with a PDMS prepolymer [RTV 615 A and B (10:1, w/w)] at 2,000 rpm for 60 s and cured at 80 ^{o}C for 10 min in an oven. The microfluidic device was ready for use after baking at 80 ^{o}C for 72 h.

Cell culture

Human umbilical vein endothelial cells (HUVEC-C, a cell line derived from primary human umbilical vein endothelial cells) and human hepatocellular carcinoma cells (HepG2) were obtained from the Chinese Academy of Sciences (Shanghai, China). Two types of cells were routinely cultured in DMEM supplemented with 10% FBS, 100 U/mL penicillin, and 100 μg/mL streptomycin in a humidified 5% CO_2 atmosphere at 37 °C. The cells were normally passaged at a ratio of 1:3 every 3 days to maintain them in the exponential growth phase. When the cells reached confluence, they were harvested through trypsinization with 0.25% trypsin in phosphate buffered solution (PBS, 0.01 M, pH 7.4) at 37 °C. Trypsinization was stopped by adding freshly supplemented DMEM. The cell

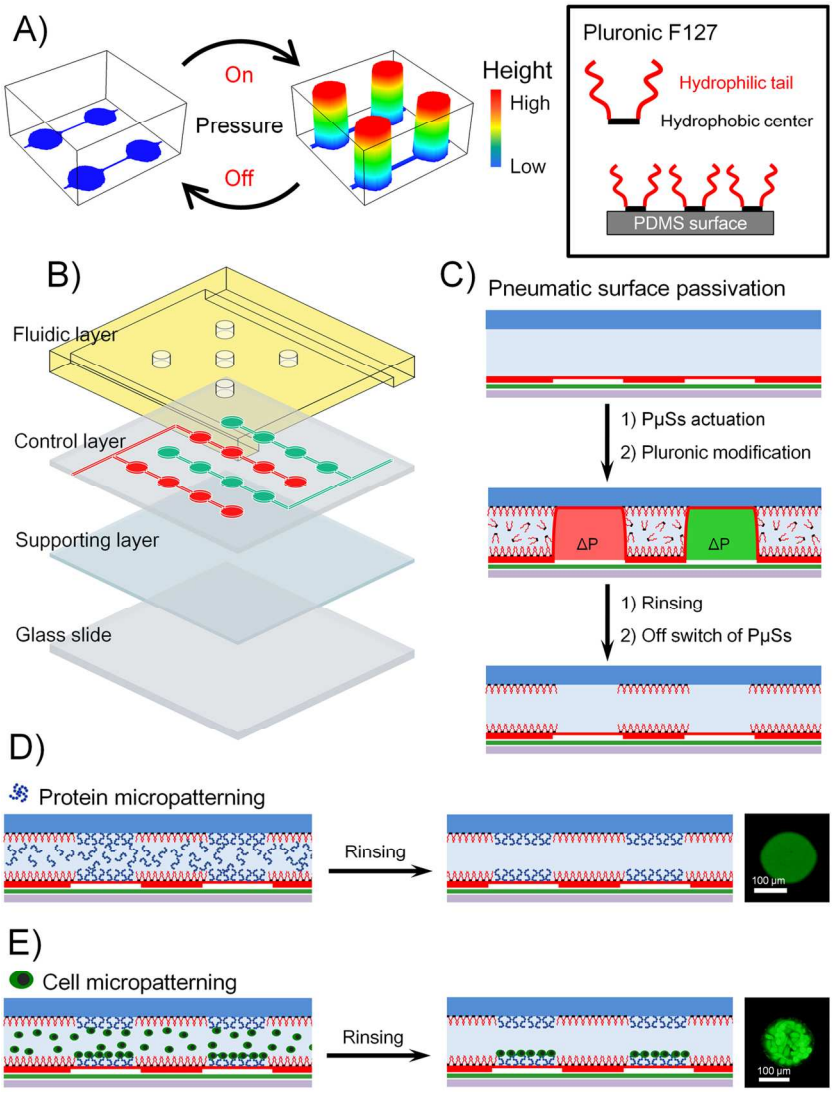

Fig. 1 Micropatterning of proteins and cells in the integrated microfluidic device by using pneumatic microstructures' (PμSs) actuation and spatially controlled surface passivation. (A) Three dimensional views of PμSs with on/off switch by gas pressure. (B) Composition of the device (the four layers are sequentially shown from top to bottom, namely, the fluidic layer, control layer, supporting layer, and glass slide). (C) PμSs-assisted surface passivation by Pluronic F127, which just modify the non-blocked region in the chamber. (D) Protein micropatterning on the PμSs-blocked surface. The fluorescent image shows FITC-labelled BSA was immobilized on the round surface corresponding to the PμSs-blocked area. (E) Cell micropatterning on the PμSs-blocking and adhesive protein-pretreated surface. HUVEC-C cells presented a well-controlled adhesion on the surface corresponding to the PμSs-blocked region. The schematic image in the square on the top right presents the feature of Pluronic F127 which has both hydrophilic and hydrophobic groups, and shows its immobilization on the PDMS surface.

suspension was centrifuged at 1000 rpm for 5 min. The cells were then resuspended in supplemented DMEM for further use.

Controllable surface passivation

Sterilization of the device was performed at the beginning of surface passivation. Microfluidic device was first rinsed by flushing 70% alcohol, ultra pure water, and PBS one after another. Thereafter, the PμSs were activated by gas pressure to generate blocked regions on the surface of the microchamber in the device. Then, a solution of 1% w/w Pluronic F127 in PBS were injected into the microfluidic device and allow to be adsorbed onto the PDMS surfaces of the microchamber. After incubation for 24 h at room temperature, the microfluidic device was washed with PBS thoroughly for at least three times and the PμSs were selectively deactivated to release the blocked regions for micropatterning.

The contact angles of PDMS surfaces before and after Pluronic coating were measured using Dropmeter 100 equipment (Maist Vision, Ningbo, China) via the sessile drop technique.[40] Each data point was based on 10 contact angle measurements at 5 different positions on the PDMS specimen.

Protein micropatterning in the micro-fluidic device

Preparation of different fluorophore-labeled proteins (BSA and CEA) was performed for significant visualization of protein localization before patterning process. BSA were labeled with FITC following the instructions of the EZ-label FITC protein labeling kit, and the CEA were labeled with A594 using the Alexa Fluro594 protein labeling kit. The labeled proteins were protected from light by covering tubes in foil, and were stored at 4 °C until use. The final concentration of the labeled proteins was totally adjusted to 1 mg/mL in PBS.

For single type of protein micropatterning, all the PμSs were switched off and FITC-BSA solutions were introduced into the Pluronic passivated microfluidic device. After 1 h incubation at 37 °C, the microchannel was washed thrice with PBS. Furthermore, while doing multiple protein micropatterning, the PμSs corresponding to the specific block regions in the chamber were switched off and the other PμSs were switched on to block the rest designated regions. FITC-BSA solutions were then injected into the microfluidic device and were allowed to immobilize onto the exposed blocking regions for 1 h at 37 °C. Following by washing with PBS for three times to flush away unimmobilized FITC-BSA, the former actuated PμSs were switched off, and the rest blocked regions were presented to contact the injected solution of 1 mg/mL A594-CEA. After incubated for 1 h at 37 °C, the microchamber was rinsed with PBS and washed three times to flush away unimmobilized A594-CEA.

Cell micropatterning in the microfluidic device

Before cell micropatterning, 200 μg/mL collagen-I solution was first introduced into the microfluidic device for 2 h-incubation at 37 °C followed by rinsing with PBS. For single type of cell micropatterning, HUVEC-C cells at a density of 1×10^6 cells/mL or HepG2 cells at a density of 5×10^6 cells/mL were loaded into microfluidic device and incubated under static culture condition for 2 h at 37 °C. Afterwards, the cell suspension was replaced by fresh medium. For clearly observation of micropatterning and viability assessment, the cells in the microfluidic device were stained with FDA (10 μg/mL in PBS), AO (10 μg/mL in PBS) and PI (10 μg/mL in PBS). Briefly, after removing the growth medium and rinsing with PBS, the FDA/PI or AO/PI staining solution flowed into the chambers, and the staining process was performed for 5 min at 37 °C. Afterward, PBS was introduced for 5 min as a final rinse.

For co-micropatterning, HUVEC-C and HepG2 cells were prestained respectively using different CellTracker dyes (10 μmol/L in fresh DMEM) before the seeding process according to the manufacturer's instructions (Invitrogen). Same manipulations to the multiple protein micropatterning, the specific group of PμSs were actuated and the others were switched off. HepG2 cells were then introduced into the microfluidic device at a density of 5×10^6 cells/mL. After 2 h incubation under static culture condition at 37 °C, fresh medium was introduced into microfluidic device to remove the non-adhering cells. After another 4 h culture, the actuated PμSs were switched off and the second type of cells (HUVEC-C) was seeded into the microfluidic device at a density of 1×10^6 cells/mL. The non-adhered cells were removed by a fresh medium rinsing after 2 h static culture condition. All the cell culture steps were performed inside the incubator. The information on the PμS control can be found in the supplementary information.

Microscopy and image analysis

Bright-field and fluorescence images were acquired using an inverted microscope (Olympus, CKX41) equipped with a charge-coupled device camera (Olympus, DP72) and a mercury lamp (Olympus, U-RFLT50). Data acquisition and measurement were performed using Image-Pro Plus 6.0 software (Media Cybernetics Inc.). The size of the blocked PμS region was determined by tracking the distinct edge of PμS and was measured using image analysis software Image Pro Plus 6.0. All the experiments in the current study were repeated at least five times. During each repetition at least 50 data were collected for statistical analysis. The statistical analysis was performed with software SPSS 12.0 (SPSS Inc.). The results and error bars in the graphs were expressed as the mean ± SD. Tests of data significance were performed using one-way ANOVA.

Results and Discussion

Device design and fabrication

To realize in situ micropatterning inside the microchamber, the pneumatic manipulation is applied here for region-specific functionalization. Generally, the operation of common pneumatic microvalves depends on the fact that PDMS is an elastomer, and is also based on the restriction of a fluidic channel by the deformation of PDMS membrane under pressure. In the past fourteen years, microvalves are particularly important as components that have enabled the design and examination of complicated microfluidic devices, and these have opened up a number of areas of application in chemistry and biology.[41,42] The on/off switch of microvalves has been used to complete various controllable microfluidic manipulations like microflow orientation, bead and cell trapping, and local protein/antibody immobilization.[36,38,43,44] As we known, the microvalves remain flat under 0 psi gas pressure, and can also deflect upwards to the top surface of microchannel while using an enough gas pressure actuation. Both the top and the bottom surface areas corresponding to the valves can be blocked and protected. This means that the spatial control of surface functionalization can be performed. Along with those excellent works aforementioned, we plan to improve and demonstrate the precise micropatterning in the microfluidic device by pneumatic component, and make its function (i.e., high throughput and shape-changeable) and application (i.e., proteins and mammalian cells) more diversified in this study.

Generally, the integrated microfluidic device in the present study is composed of four layers (Fig. 1 and Fig. S1, ESI†): the fluidic layer, the control layer, the supporting layer, and a glass slide. In detail (Fig. S2–Fig. S7, ESI†), the fluidic layer, with micrometer-scaled component, contained an individual chamber for protein and cell staying. To prevent chamber collapse during the experiment, a set of micropillar arrays was specifically and optimally arranged in the chamber (Fig. S2–Fig. S7, ESI†). The inlet and outlet were set at the both ends of the chamber respectively, and were used for liquid injection, chamber purging, protein and cell loading and waste exclusion. The control layer consisted of two sets of water-filled channel networks incorporated pneumatic microstructures (PμSs) in their middles or terminals. The PμS arrays were independently controlled by external gas pressure (For the information on PμS control, see the supplementary information, ESI†). Different from the common valves (i.e., size similar to the channel) in microfluidic chips, the size of the PμSs here is much smaller than the size of microchamber (For the detailed dimension of all the devices used in the current study, see Fig. S2–Fig. S7, ESI†). When pressure is applied, the membrane of the PμSs deflects upwards to the top surface of the fluidic chamber, creating the blocked regions, which can be reversibly and real-time controlled through on/off switch of pneumatic actuation (Fig. 1A and Fig. S8, ESI†). Finally, the supporting layer coated on the glass slide was employed for irreversible seal of the channel networks in the control layer.

Surface passivation and micropatterning

The hydrophobicity of PDMS tends to promote nonspecific protein adsorption (biofouling).[45] For micropatterning of

biological substances, it is essential to create bio-inert regions on the microchamber surface except the PμSs-blocked surface before the biological substances deposit. Although the use of covalently grafted polymer to modify PDMS has been proposed to create robust coatings with tunable chemistry and precise local definition, the methods reported so far are relatively complex to implement and difficult to integrate with microfluidic chips.[46,47] Alternatively, physically adsorbed polymer coatings appear as an interesting approach to covalent ones since the coating process can be easily implemented inside a microfluidic device.[48] Among the possible candidates, a group of PEO-based triblock polymers (such as Pluronics) has been proven to be especially suitable for the prevention of protein adsorption and cell attachment.[49-51] The mechanism contributing to this capability is generally attributed to its hydrophilicity, flexibility, chain mobility, and high steric exclusion volume in water.[49] Pluronics, with the general composition of $(PEO)_m(PPO)_n(PEO)_m$ (for Pluronic F127, m = 100, n = 65, molecular weight = 12,600), has been widely used in many biotechnological applications because of its extremely low toxicity and immunogenic response.[51] Thus, Pluronic was chosen as blocking agent to passivate the non-blocked regions in this study. This class of polymers have poly(propylene oxide) (PPO) centers with poly(ethylene oxide) (PEO) side chains (Fig. 1 and Fig. S9, ESI†). The PPO domain adsorbs quasi-irreversibly to hydrophobic surfaces, creating a surface coating of PEO chains. Fig. 1C schematically depicts the bio-inert modification of the non-blocked region using Pluronic F127. The PμSs were firstly actuated to protect the blocked spots and then the whole microchamber was incubated with the Pluronic solution. Since non-blocked regions could access liquid freely, Pluronic molecules could interact with the PDMS surface of these regions through hydrophobic interaction and then form a poly(ethylene oxide) (PEO) covered layer in the microchamber. Due to the difference in liquid access between non-blocked regions and blocked regions, the localized anti-adhesive domains can be easily created in non-blocked regions. Meanwhile, the wettability of Pluronic-treated surface was evaluated through contact angle, which was believed to play an important role in controlling surface hydrophilization. The result (Fig. S9, ESI†) showed that the contact angle decreased after coating with Pluronic. This indicates that the wettability of PDMS surface increased after coating. Although this increase of wettability is lower than the one obtained

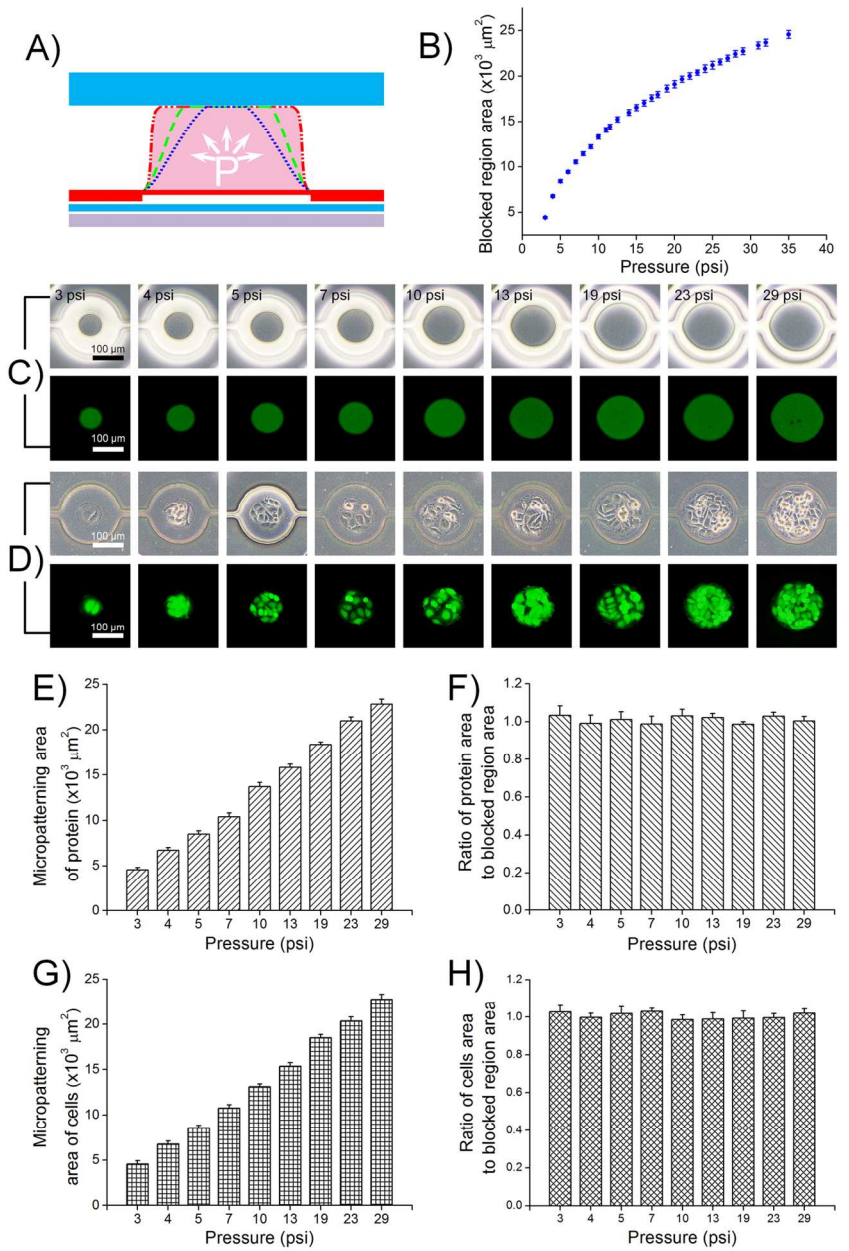

Fig. 2 Dynamic investigation of PμS manipulation and micropatterning of proteins and cells at different gas pressures. (A) Sectional view of PμS deformation dynamics by changing gas pressures. (B) Quantification of PμS blocking dynamics at various gas pressures. The blocked area between the PμS and the top surface of microchamber was applied for quantitative assessment. (C) The optical images of PμS-blocked regions (top) and the fluorescent images of FITC-labelled BSA micropatterning (bottom) at various gas pressures. (D) The optical images of HUVEC-C cell micropatterning (top) and the fluorescent images of micropatterning of HUVEC-C cell stained by FDA/PI solution (bottom). (E) Micropatterning area of BSA at various gas pressures. (F) Ratio between the BSA patterned area and PμS-blocked area. (G) Micropatterning area of HUVEC-C cells at various gas pressures. (H) Ratio between the HUVEC-C cell patterning area and PμS-blocked area. The pressures used in (D) are corresponding to the pressures in (C).

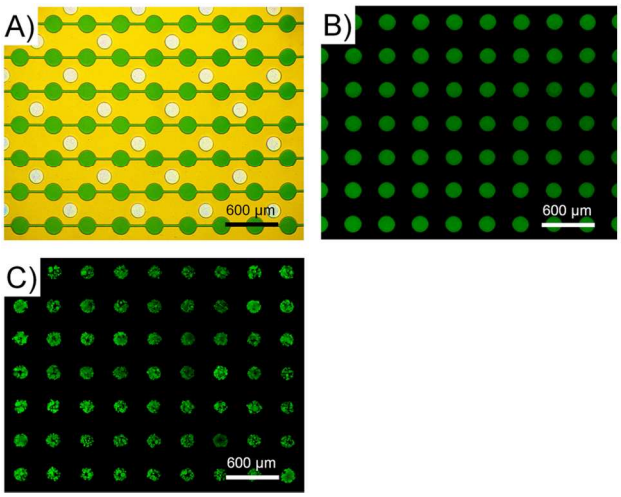

Fig. 3 High throughput micropatterning using the PμS array. (A) The optical image of PμS array. Microchannel network in the control layer was loaded with green food dye for visualization of the PμSs. (B) Array-like micropatterning of FITC-labeled BSA in the chamber. (C) Array-like micropatterning of HepG2 cells (AO/PI staining) in the chamber. These results suggest that both proteins and cells can be localized by using the PμS array in a high throughput way.

after oxygen plasma or UV/O_3 treatment of PDMS,[52,53] the results are in the typical range of the hydrophilization achieved after the surface treatment of hydrophobic surfaces using physisorbed polymers.[54,55]

Further, the protein and cell loading/positioning tests were performed to investigate the effect of Pluronic treatment and the feasibility of pneumatic micropatterning in a wide range of biological applications. For protein micropatterning, FITC-labeled BSA was introduced into the microchamber. Albumin was used because of its abundance in human blood and its strong adhesion tendency. Fig. 1D showed that FITC-BSA selectively adsorbed to the areas of the blocked regions and non-staying on the Pluronic-treated surfaces. Meanwhile, the cell micropatterning also presented the similar results (Fig. 1E). After the loading and rinsing processes, the cells were spatially immobilized on the surface of the blocked region pretreated with the cell adhesive protein. Clearly, the adhered cells on the surface of the blocked regions formed a well-restricted micropatterning shape. The results suggest that the micropatterning method has the ability to position cells inside a microfluidic device with control over their spatial arrangement. Meanwhile, the effect of Pluronic in anti-protein absorption and anti-cell adhesion was demonstrated. These results demonstrated that the pneumatic micropatterning cooperated with Pluronic-assisted surface passivation works for the in situ localization of both protein molecules and mammalian cells in microfluidics.

The deformation of the PDMS membrane was affected by the applied pneumatic pressure, which could further affect the area of the blocked regions. Thus, the spatial appearance dynamics of the PμSs was first evaluated correspondingly by subjecting them to varied gas pressures (Fig. 2). In the current study, we tested a range of pneumatic actuation from 0 psi to 35 psi (a pressure range that could keep the device integrity and prevent leakage) for the systematic characterization of PμS-assisted blocking dynamics. As expected, the PDMS membrane showed positive deformation along with the increase of gas pressure (Fig. 2B), which resulted in the enlargement of the blocked area on the surface of microchamber. These results implied that the size-modulated bio-micropattern could be realized in the microchamber through pressure control. Furthermore, a quantitative immobilization of FITC-BSA and HUVEC-C cells onto the blocked surface was performed respectively under various gas pressures. Fig. 2C and 2E showed that the protein micropatterning area was increased positively along with the change of the applied pressures, which was also consistent with the tendency of the deformation of PDMS membrane. Same to the tendency of protein micropatterning, the micropatterned cell area also increased with increasing pressure (Fig. 2D and 2G). The blocked regions were covered with the adhered cells varying from several cells to dozens of cells, which suggested that this type of PμS-assisted micropatterning method could realize cell localization at single cell level. Meanwhile, the multi-quantity of cell micropatterning can be performed by using dynamically controlled PμSs in the device. Further, the assessment of geometrical consistency between the blocked regions and the protein/cell immobilized areas was performed, respectively. The area ratio between the blocked regions and protein/cell patterning regions was used for quantitative comparison. The results (Fig. 2F and 2H) showed that the areas of both

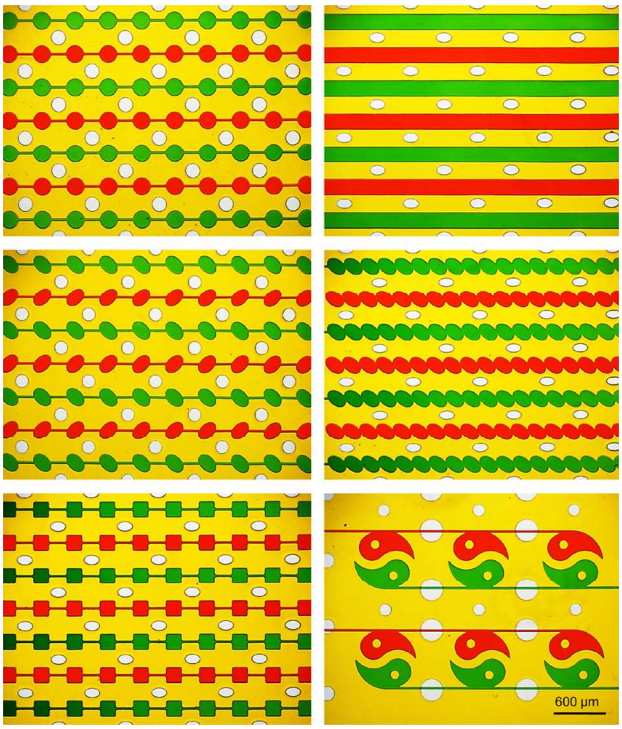

Fig. 4 The shape-diversified PμSs in the microfluidic devices. Totally, six types of PμSs were prepared in this study, such as round, strip, oval, wavy, square, and Taiji-shaped PμSs. Two sets of PμSs in the devices were marked respectively by green and red food dyes.

micropatterned proteins and cells presented well-defined geometry corresponding to the blocked regions. Totally, these results suggested that the size modulation of both protein and cell micropatterning could be carried out by pressure-regulated PμSs in the microfluidic device, and the generated protein/cell micropatterning on the surface of the chamber faithfully reproduced the geometric property of PμS-blocked region.

Protein/cell micropatterning in a high throughput and geometric diversity way

Micropatterning has the feature of manipulating a large quantity of homotypic samples and controlling their spatial configuration. Therefore, further experimental investigation of pneumatic micropatterning in the device integrated with PμS array (Fig. 3A) was performed to achieve a feasible control of bio-component (proteins and cells) localization in a high throughput and geometry-controlled manner. To perform protein micropatterning, the PμS arrays were all switched off and kept at a non-actuated status to expose the blocked regions. The FITC-labeled BSA solution was then introduced into the Pluronic-pretreated chamber, and incubated for a while following by rinsing. The results showed that a large number of proteins arranged on the surface of the blocked areas, which formed a stable spotted array of proteins (Fig. 3B). The protein arrays are known as a good platform for high throughput study of various protein-related interactions, as well as different immunoassays.[56,57] The PμS array-based cell micropatterning was also performed in the microfluidic chamber. HepG2 cells were loaded into the device and selectively immobilized on the collagen-pretreated surface. The rinsing process removed the rest cells suspended in the chamber. As shown in Fig. 3C, HepG2 cells completely adhered on the surface of the collagen-treated spot array, and were organized as a shape-controlled cell population with high viability (no dead cells were observed during this test). This result demonstrated that the well-defined cell array was successfully accomplished by using the PμSs integrated in the microfluidic device, which would be much helpful for high throughput cell assay and analysis.

Meanwhile, the exploration of geometric diversity of pneumatic micropatterning was carried out. For this purpose, we designed and fabricated six types of microfludic devices with different shape of PμSs, including round, strip, square, oval, Taiji-shaped, and wavy (Fig. 4, and Figs. S2-S7, ESI†). Based on the PμSs control and Pluronic modification, the protein (BSA) and cell (HUVEC-C and HepG2) micropatterning were performed respectively in these devices. Fig. 5A showed that FITC-labeled BSA exhibited uniformly fluorescent shape in the microchamber, almost corresponding to what the PμSs look like. Similarly, two types of cell populations also presented a controlled adhesion in the blocked regions with different shapes, corresponding to the type of PμSs geometry (Fig. 5B and 5C, and Fig. S10, ESI†). These results suggested that the spatial appearance of both protein and cell micropatterning in the device could be precisely controlled by using the well-designated PμSs, and demonstrated that this micropatterning method had the ability of producing a high quality of protein localization and cell organization.

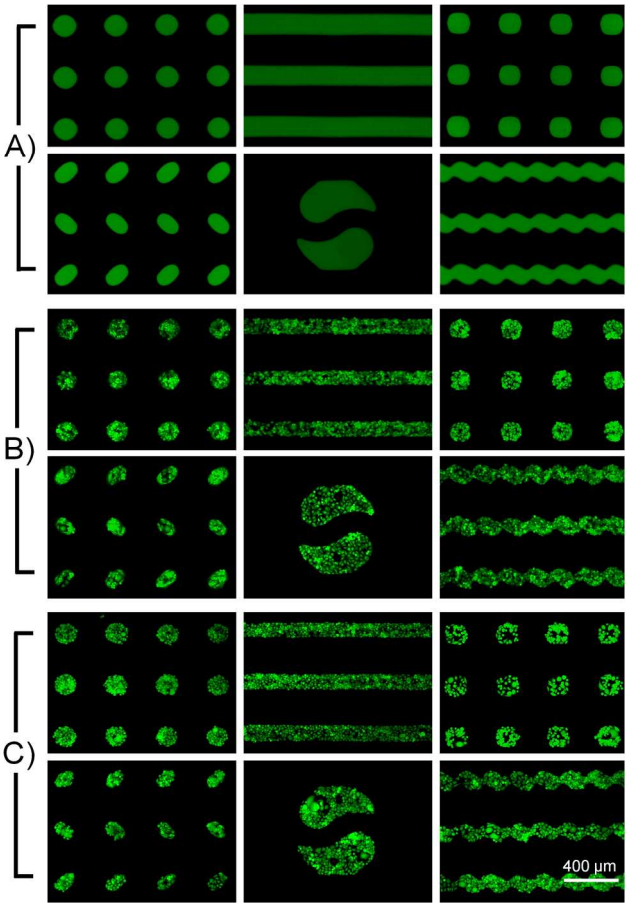

Fig. 5 Geometry-controlled micropatterning by different well-designed PμSs. (A) The fluorescent images of BSA micropatterning using different PμSs. (B) The fluorescent images of HUVEC-C cell micropatterning using different PμSs. (C) The fluorescent images of HepG2 cell micropatterning using different PμSs.

PμSs-based protein/cell co-micropatterning

In this section, we demonstrated the applicability of this pneumatic method for in situ micropatterning multiple biological substances. The sequentially controllable manipulations of PμSs were applied to carry out the biological co-micropatterning in the device (Fig. S11, ESI†). After bio-inert surface modification of the non-blocked regions in the microchamber, one set of PμSs was depressurized to expose the blocked regions for the bio-component solution accessing, and the other PμSs remained actuation to keep the rest of the blocked regions from liquid accessing. Thereafter, the first biological component was introduced into the microchamber and selectively immobilized onto the exposed blocking regions. Subsequently, the second bio-component micropatterning was obtained by the same process after off switch of another set of the PμSs. The in situ micropatterning of multiple biological components inside the microfluidic device can be performed through successively modulating the on/off switch of the PμSs

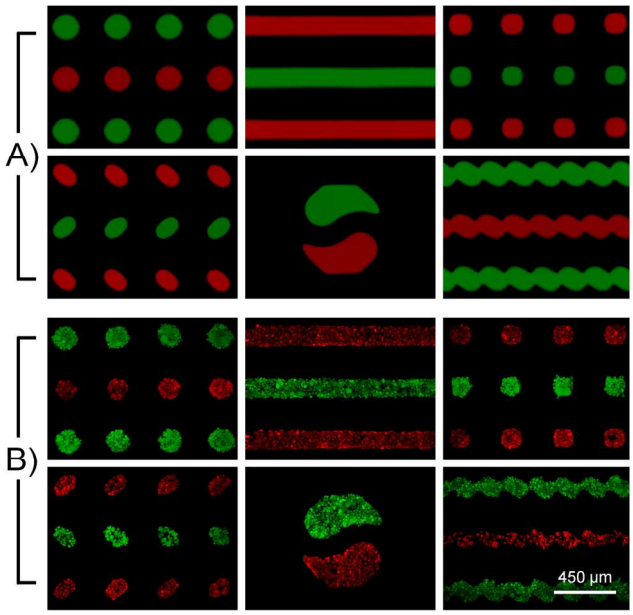

Fig. 6 Co-micropatterning of different proteins/cells using PμSs. (A) Immobilization of both FITC-labelled BSA and Alexa Fluro594-labelled CEA with various shapes in the same chamber. (B) Localization of both HUVEC-C cells (red) and HepG2 cells (green) with various shapes in the same chamber.

without using external devices or complex fabrication process, which provides a simple and compatible method to achieve co-micropatterning inside the microfluidic device.

In the current study, the micropatterning of multiple proteins (BSA and CEA) and cells (HUVEC-C and HepG2) was respectively constructed by using this method. The results (Fig. 6A) showed that the multiple micropatterning of proteins with varied shapes were fabricated by successively operating the PμSs. The spatial micropatterning of multiple proteins inside the microchamber could potentially broaden the application of this microfluidic pneumatic method in the studies of protein interactions and immunoassays. Furthermore, the results presented the cell co-micropatterning can also be accomplished inside the microfluidic chamber (Fig. 6B and Fig. S12, ESI†). The micropatterned cell populations presented well-defined geometry with various shapes. HUVEC-C and HepG2 cells were respectively localized at the specifically defined regions without contamination between each other. This suggests that the PμSs-assisted method allows for the micropatterning of multiple cell types, with high control performance of the spatial arrangement of cells. The ability of engineering micropatterning of multiple types of living cells allowed implementation of complex microenvironment for quantitative biological assessment, which indicated that the potential use of the pneumatic micropatterning in many cellular studies such as wound healing, stem cell differentiation, and tumor metastasis.

Conclusions

In this study, we presented an in situ micropatterning approach for high throughput and multiplex localization of proteins and mammalian cells by using pneumatic switch and controllable surface passivation in a microfluidic device. The pneumatic microstructures can conveniently realize the multi-quantity of protein/cell immobilization in the well-defined regions based on their precise-controlled dimensional dynamics. Meanwhile, the PμSs can accomplish the array-like micropatterning operation of multiple biological components in the device, which could be a new preparation for high-throughput biology. Further, the well-designed PμSs have the ability to simply realize the geometric diversity of protein/cell localization. More importantly, we demonstrated that multi-types of proteins and cells could be co-patterned with shape-regulated arrangement on the defined surfaces of microchamber in the microfluidic device, which would contribute to several multifactor-involved biological studies like protein interaction, cell coculture and communication, and tissue simulation. Additionally, the on-chip integration of PμSs-assisted micropatterning is potentially useful for the development of various microfluidic high-throughput screening, clinical diagnosis, and immunosensor.

Acknowledgements

This study was supported by the National Natural Science Foundation of China (21375106, 21175107 and 31100726), the Fundamental Research Funds for the Central Universities of China (Z109021303), and the Northwest A&F University.

Notes and references

[a] Colleges of Science and Veterinary Medicine, Northwest A&F University, Yangling, Shaanxi 712100, China. Tel: +86-298-708-2520; E-mail: jywang@nwsuaf.edu.cn.
[b] Energy Research Institute of Shandong Academy of Sciences, Jinan, Shandong 250014, China.
[c] School of Materials Science and Engineering, Northwestern Polytechnical University, Xi'an, Shaanxi 710072, China.

† Electronic Supplementary Information (ESI) available: PμS control and supplementary Fig. S1–S12 about PμSs-assisted micropatterning of biological components in the microfluidic device. See DOI: 10.1039/b000000x/

1 L. Gervais, N. de Rooij and E. Delamarche, *Adv. Mater.*, 2011, **23**, H151-H176.
2 M. Théry, *J. Cell Sci.*, 2010, **123**, 4201-4213.
3 J. Deeg, M. Axmann, J. Matic, A. Liapis, D. Depoil, J. Afrose, S. Curado, M. Dustin and J. Spatz, *Nano Lett.*, 2013, **13**, 5619-5626.
4 K Okano, A. Matsui, Y. Maezawa, P. Hee, M. Matsubara, H. Yamamoto, Y. Hosokawa, H. Tsubokawa, Y. Li, F. Kao and H. Masuhara, *Lab Chip*, 2013, **13**, 4078-4086.
5 U. Vermesh, O. Vermesh, J. Wang, G. Kwong, C. Ma, K. Hwang and J. Heath, *Angew. Chem. Int. Ed.*, 2011, **50**, 7378-7380.
6 B. Manz and J. Groves, *Nat. Rev. Mol. Cell. Biol.*, 2010, **11**,342-352.
7 M. Cretich, F. Damin and M. Chiari, *Analyst*, 2014, **139**, 528-542.
8 T. Fernandes, M. Diogo, D. Clark, J. Dordick and J. Cabral, *Trends Biotechnol.*, 2009, **27**, 342-349.
9 X. Mu, W. Zheng, J. Sun, W. Zhang and X. Jiang, *Small*, 2013, **9**, 9-21.

10 Y. Liu, H. Li, S. Yan, J. Wei and X. Li, *Biomacromolecules*, 2014, **15**, 1044-1054.
11 C. Tan, B. Seo, D. Brooks, E. Chandler, H. Craighead and C. Fischbach, *Integr. Biol.*, 2009, **1**, 587-594.
12 E. Felton, C. Copeland, C. Chen and D. Reich, *Lab Chip*, 2012, **12**, 3117-3126.
13 M. Kim, J. Choi, H. Jung, J. Katz, M. Kim and J. Doh, *Langmuir*, 2010, **26**, 12112-12118.
14 D. Lee and S. Yang, *ACS Appl. Mater. Interfaces*, 2013, **5**, 2658-2668.
15 B. Yuan, Y. Jin, Y. Sun, D. Wang, J. Sun, Z. Wang, W. Zhang and X. Jiang, *Adv. Mater.*, 2012, **24**, 890-896.
16 W. Kim, M. Jang, S. Joo, W. Sun and Y. Nam, *Lab Chip*, 2014, **14**, 799-805.
17 A. Yusof, H. Keegan, C. Spillane, O. Sheils, C. Martin, J. O'Leary, R. Zengerle and P. Koltay, *Lab Chip*, 2011, **11**, 2447-2454.
18 H. Lee, S. Park, Y. Kang, S. Jeong, S. Choi, K. Jahng and C. Cho, *Acta Biomater.*, 2010, **6**, 519-525.
19 N. Rodriguez, R. Desai, B. Trappmann, B. Baker and C. Chen, *Langmuir*, 2014, **30**, 1327-1335.
20 D. Barrett and M. Yousaf, *Angew. Chem. Int. Ed.*, 2007, **46**, 7437-7439.
21 S. Zhao, A. Chen, A. Revzin, T. Pan, *Lab Chip*, 2011, **11**, 224-230.
22 D. Chiu, N. Jeon, S. Huang, R. Kane, C. Wargo, I. Choi, D. Ingber, G. M. Whitesides, *Proc. Natl. Acad. Sci. U. S. A.*, 2000, **97**, 2408-2413.
23 G. M. Whitesides, *Nature*, 2006, **442**, 368-373.
24 C. Zheng, L. Zhao, G. Chen, Y. Zhou, Y. Pang and Y. Huang, *Anal. Chem.*, 2012, **84**, 2088-2093.
25 M. Zhou, H. Ma, H. Li and J. Qin, *Biomaterials*, 2014, **35**, 1390-1401.
26 J. Wu, Q. Chen, W. Liu, Y. Zhang and J. Lin, *Lab Chip*, 2012, **12**, 3474-3480.
27 P. Tabeling, *Curr. Opin. Biotechnol.*, 2014, **25**, 129-134.
28 A. Khademhosseini, K. Suh, S. Jon, G. Chen, G. Eng, J. Yeh, R. Langer. *Anal. Chem.*, 2004, **76**, 3675-3681.
29 M. Kim, K. Song and J. Doh, *Colloids Surf. B Biointerfaces*, 2013, **112**, 134-138.
30 C. Priest, *Biomicrofluidics*, 2010, **4**, 32206.
31 S. Hu, X. Ren, M. Bachman, C. Sims, G. Li and Allbritton, N. Allbritton, *Anal. Chem.*, 2004, **76**, 1865-1870.
32 J. Atencia and D. Beebe, *Nature*, 2005, **437**, 648-655.
33 T. Didar and M. Tabrizian, *Lab Chip*, 2012, **12**, 4363-4371.
34 S. Allazetta, S. Cosson and M. Lutolf, *Chem. Commun.*, 2011, **47**, 191-193.
35 J. Garcia-Cordero and S. Maerkl, *Chem. Commun.*, 2013, **49**, 1264-1266.
36 C. Zheng, J. Wang, Y. Pang, J. Wang, W. Li, Z. Ge and Y. Huang, *Lab Chip*, 2012, **12**, 2487-2490.
37 J. Wang, G. Sui, V. Mocharla, R. Lin, M. Phelps, H. Kolb and H. Tseng, *Angew. Chem. Int. Ed.*, 2006, **45**, 5276-5281.
38 W. Liu, L. Li, X. Wang, L. Ren, J.-C. Wang, Q. Tu, X. Huang and J. Wang, *Lab Chip*, 2010, **10**, 1717-1724.
39 L. Li, L. Ren, W. Liu, J.-C. Wang, Y. Wang, Q. Tu, J. Xu, R. Liu, Y. Zhang, M. Yuan, T. Li and J. Wang, *Anal. Chem.*, 2012, **84**, 6444-6453.
40 P. Ferraro, S. Coppola, S. Grilli, M. Paturzo and V. Vespini, *Nat. Nanotechnol.*, 2010, **5**, 429-435.
41 S. Suri, A. Singh, A. H. Nguyen, A. M. Bratt-Leal, T. C. McDevitt and H. Lu, *Lab Chip*, 2013, **13**, 4617-4624.
42 H. Fan, W. Gu, J. Wang, Y. J. Blumenfeld, Y. Y. El-Sayed and S. Quake, *Nature*, 2012, **487**, 320-324.
43 W. Liu, L. Li, J.-C. Wang, Q. Tu, L. Ren, Y. Wang and J. Wang, *Lab Chip*, 2012, **12**, 1702-1709.
44 Z. Fu, G. Shao, J. Wang, D. Lu, W. Wang and Y. Lin, *Anal. Chem.*, 2011, **83**, 2685-2690.
45 D. Kim and A. Herr, *Biomicrofluidics*, 2013, **7**, 41501.
46 Q. Pu, O. Oyesanya, B. Thompson, S. Liu and J. Alvarez, *Langmuir*, 2007, **23**, 1577-1583.
47 T. Rohr, D. F. Ogletree, F. Svec and J. M. J. Fréchet, *Adv. Funct. Mater.*, 2003, **13**, 264-270.
48 K, Perez-Toralla, J. Champ, M. Mohamadi, O. Braun, L. Malaquin, J. Viovy and S. Descroix, *Lab Chip*, 2013, **13**, 4409-4418.
49 V. Liu, W. Jastromb, S. Bhatia, *J. Biomed. Mater. Res.*, 2002, **60**, 126-134.
50 Y. Li, A. J. Keefe, M. Giarmarco, N. Brault and S. Jiang, *Langmuir*, 2012, **28**, 9707-9713.
51 Z. Wu and K. Hjort, *Lab Chip*, 2009, **9**, 1500-1503.
52 S. Tan, N. Nguyen, Y. Chua and T. Kang, *Biomicrofluidics*, 2010, **4**, 032204.
53 K. Ma, J. Rivera, G. Hirasaki and S. Biswal, *J. Colloid. Interface Sci.*, 2011, **363**, 371-378.
54 C. Kuo, C. Chiang, R. Y. Huang, H. Lee and A. Wo, *NPG Asia Mater.*, 2012, **4**, e27.
55 T. Yasui, M. Mohamadi, N. Kaji, Y. Okamoto, M. Tokeshi and Y. Baba, *Biomicrofluidics*, 2011, **5**, 44114.
56 L. Berrade, A. Garcia and J. Camarero, *Pharm. Res.*, 2011, **28**, 1480-1499.
57 M. Hartmann, J. Roeraade, D. Stoll, M. Templin and T. Joos, *Anal. Bioanal. Chem.*, 2009, **393**, 1407-1416.

Graphical Abstract

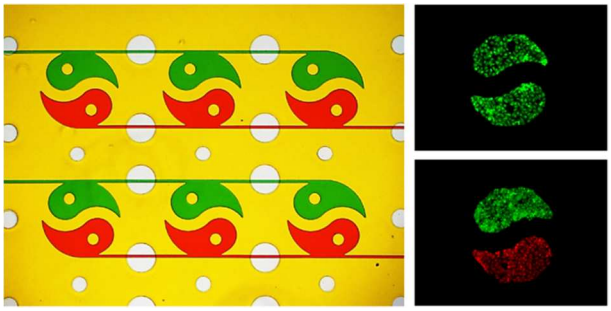

We present a micropatterning method for protein/cell localization by using pneumatically controllable microstructures in an integrated microfluidic device.